processes

MDPI

Article

Valuable Biodiesel Catalyst from Solvay Wastewater

Mai Hassan Roushdy * and Rana Adel Bayoumi

Chemical Engineering Department, Faculty of Engineering, The British University in Egypt,
El-Sherouk City 11837, Egypt; rana.adel@bue.edu.eg
* Correspondence: mai.hassan@bue.edu.eg

Abstract: Biodiesel is considered a renewable, green fuel as it is derived from renewable living resources like animal fats or vegetable oils. This research is utilized to investigate the possibility of using Solvay wastewater as a source of biodiesel catalyst, which is CaO. $CaCl_2$ from Solvay wastewater reacts with CO_2 to produce $CaCO_3$. $CaCO_3$ is then heated to produce pure CaO. Waste cooking oil, wastewater, and CO_2, which are considered dangerous materials to the environment, are used to produce valuable products. This research has environmental and economic benefit benefits of using waste materials as a replacement for raw materials. The selected experimental parameters for the $CaCO_3$ production step are stirring rate (500–1300) rpm, CO_2 gas flow rate (900–2000) mL/min, amount of ammonia (15–35) mL, and glycerol volume (0–25) mL. The selected experimental parameters for the biodiesel production step are reaction time (2–6) h, methanol to oil ratio (9–15), catalyst loading (1–5) %, and reaction temperature (50–70) °C. The impact of reaction parameters on reaction responses was assessed using the response surface methodology technique. A formula that represents the reaction response as a function of all the independent factors has been created. The optimization of the process is done in two steps: the first one is for the $CaCO_3$ process while the second one is biodiesel production optimization. The first optimization was done to get the $CaCO_3$ with minimum particle size and yield. The second optimization was done to get the maximum amount of biodiesel using minimum energy and low reaction conditions. Process optimization resulted in another economic benefit for this research. The resulted biodiesel yield equals 95.8% biodiesel yield at 2 h reaction time, 15:1 molar ratio of methanol to oil, 56 °C reaction temperature, and 1% catalyst loading.

Keywords: biodiesel; solvay wastewater; CaO; response surface methodology; optimization

check for updates

Citation: Roushdy, M.H.; Bayoumi, R.A. Valuable Biodiesel Catalyst from Solvay Wastewater. *Processes* **2022**, *10*, 1042. https://doi.org/10.3390/pr10051042

Academic Editors: Cataldo De Blasio and Gabriel Salierno

Received: 7 April 2022
Accepted: 20 May 2022
Published: 23 May 2022

1. Introduction

The constant rise in energy need for global industrialization and modernization has resulted in a non-renewable energy shortage in recent years. Because energy is such an important aspect globally, people are becoming more aware of the need to find environmentally friendly biofuels [1–3]. Biofuels like biodiesel are considered effective renewable sources. Transesterification is one of the processes that produce biodiesel. Biodiesel, commonly known as fatty acid methyl diesel, is chemically identical to Petro-diesel as they have approximately the same properties. Biodiesel is made by mixing biomass, ethanol or methanol, and catalysts such as sodium or potassium hydroxide or solid catalyst. Biomass is like vegetable oils and animal fats [4–7].

To start the transesterification process, chemical or biological catalysts are used. Homogeneous reagents (alkali or acid), heterogeneous agents (solid acid or solid alkali catalysts), heterogeneous nano-catalysts, and supercritical fluids make up the chemical catalyst. These catalysts are effective in completing the process, even though the reaction requires a lot of energy and a long purification step to get the refined end product [8–10].

Many researchers used CaO or solid waste containing CaO as a biodiesel catalyst. Watcharathamrongkul et al. used calcium oxides produced from the calcination of CaO,

$Ca(OH)_2$, limestone, and $Ca(OH)_2/CaO$ as solid base catalysts to catalyze the transesterification of soybean oil and ethanol. After 10 h of reaction time, the conversion of soybean oil reached 96.3 percent [11]. Calcium oxide (CaO) was generated from eggshells and employed as a catalyst for biodiesel generation from rubber seed oil with 99.7% yield by Sai Bharadwaj et al. With a 12:1 molar ratio of methanol to rubber seed oil, 4% by weight catalyst, and a 3 h reaction duration, 99.7% RSO to biodiesel conversion was achieved [12]. As a heterogeneous catalyst, Al-Sakkari et al. used cement kiln dust. The following circumstances were discovered to be optimal: a reaction period of around 6 h, catalyst loading of 2% of oil mass, and methanol to oil molar ratio of 15:1. In all trials, a fixed mixing speed of 800 rpm and a constant temperature of 65 °C were used [13].

The Solvay process's basic product is synthetic soda ash (Na_2CO_3) as described in Figure 1. Soda ash is an important raw material source for a variety of industries. In the Solvay process, ammonia is recovered. The liquid waste solution of the soda production remains after the ammonia has been removed. In soda ash production through the Solvay process, a waste stream of 10 m^3 per ton of product Na_2CO_3 is produced. This stream, known as distiller waste, contains $CaCl_2$, NaCl, and small quantities of $Ca(OH)_2$ and $CaCO_3$. This stream is discharged into the Mediterranean sea, rivers, and lakes, which cause environmental problems [14–16].

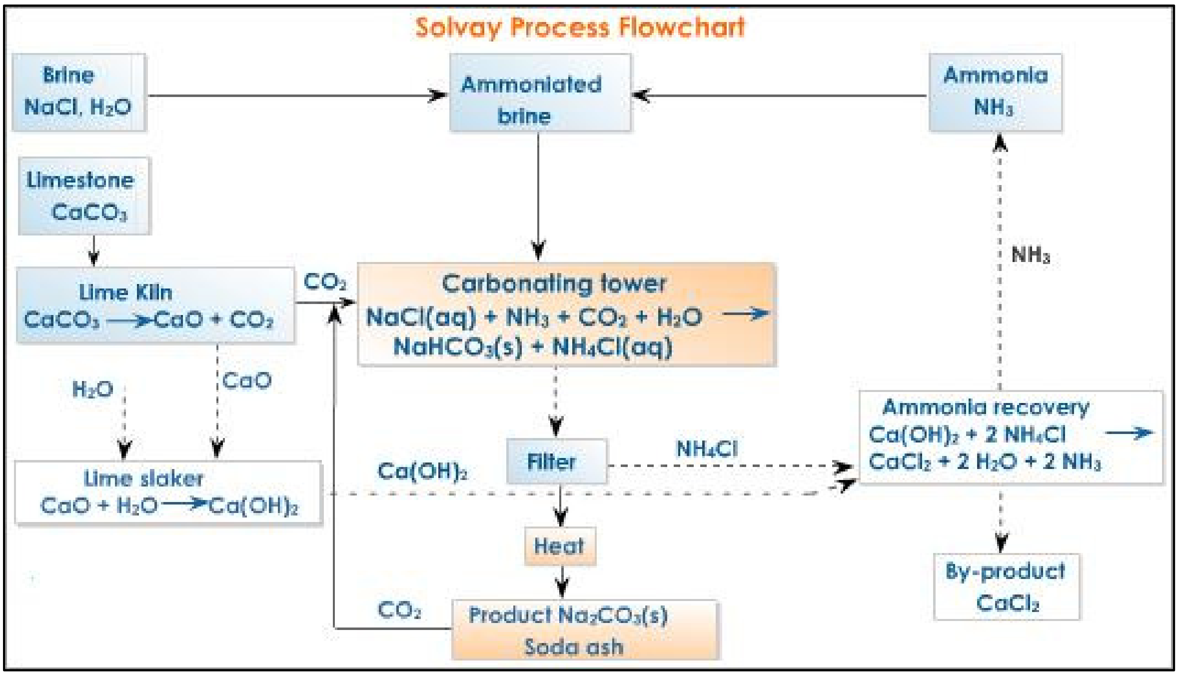

Figure 1. Solvay process.

The first goal of this research is to innovate and examine the possibility of using Solvay wastewater as a source of valuable biodiesel catalyst, which is CaO to be used as a heterogeneous catalyst using optimum process and reaction parameters. This research has an economic benefit as it used minimum energy and low reaction conditions. The second goal is using the waste cooking oil, wastewater, and CO_2 which are considered dangerous materials to the environment for producing a valuable product, so this research has an environmental benefit and economic benefit because using waste materials as a replacement for raw materials. The third goal is the production of biodiesel with a high yield, which is considered an important biofuel and can replace diesel fuel in all its uses. In the future, all petroleum products will disappear as they are non-renewable energy sources and will be replaced by renewable energy sources.

2. Materials and Methods

2.1. Experimental Work Raw Materials

There are five types of raw materials used in this work as follows:

(a) Solvay wastewater from the Solvay process factory. The composition of this wastewater is shown in Table 1.
(b) Carbon dioxide gas purchased from "Delta Carbon for Gases Company"
(c) Ammonia Solution (NH_4OH) 33% purchased from "El Nasr Pharmaceutical Chemicals company".
(d) Sunflower Waste cooking oil (SFWCO) was collected from Egyptian cafes. Table 2 lists the WCO chemical properties. Its physicochemical properties were determined using the same method used by Roushdy [9], and these properties are listed in Table 3.
(e) Methanol (MeOH) 99% that was purchased from Morgan Chemical Ltd., City, Egypt.

Table 1. Composition of Solvay wastewater.

Element	Concentration, (Kg/m^3)
$CaCl_2$	115
NaCl	54
$Ca(OH)_2$	9
$CaCO_3$	12
$CaSO_4$	4
SiO_2	1
NH_3	0.02

Table 2. Chemical composition of SFWCO.

Fatty Acid	*v*/*v* %
Arachidic acid	1.42
Eicosadienoic acid	0.43
Heptadecanoic acid	36.55
Lauric acid	0.3
Linoleic acid	1.51
Linolenic acid	2.25
Myristic acid	0.75
n-pentadecanoic acid	1.64
Oleic acid	30.44
Others	4.13
Palmitic acid	20.21
Palmitoleic acid	0.37

Table 3. Physicochemical properties of SFWCO.

Property	Value
Acid value (mg of KOH/g of oil)	1.5
Density of 25 °C (kg/m^3)	845
Molecular weight	830.2
Viscosity at 40 °C	40.3

2.2. Assessment of Produced $CaCO_3$ and the Biodiesel Catalyst (CaO)

The phases included in the substrate can be seen using X-ray diffraction (XRD). The particle size distribution was determined using the standardized screening process described in ASTM D 422/2007 [17] and ASTM E 11/2009 [18]. Scanning electron microscopes are used to show the phases and the shape of the particles present in the used biodiesel catalyst.

2.3. SFWCO Collection and Preparation

Several cafes provided SFWCO. The SFWCO was dried at 105 °C for 2 h for water removal and centrifuged for removal of any suspended materials to get clean oil for biodiesel production with high and good quality [19].

2.4. Biodiesel Catalyst Preparation (CaO)

The production of biodiesel catalyst from Solvay wastewater was done by the following steps and the experimental setup is shown in Figure 2:

1. Ammonia solution was added with a certain amount to the Solvay wastewater to form a mixture of 250 mL.
2. Glycerol was added with a certain amount to the reaction mixture, which is mixed using a magnetic stirrer (WiseStir MSH-20D) adjusted to the required stirring rate.

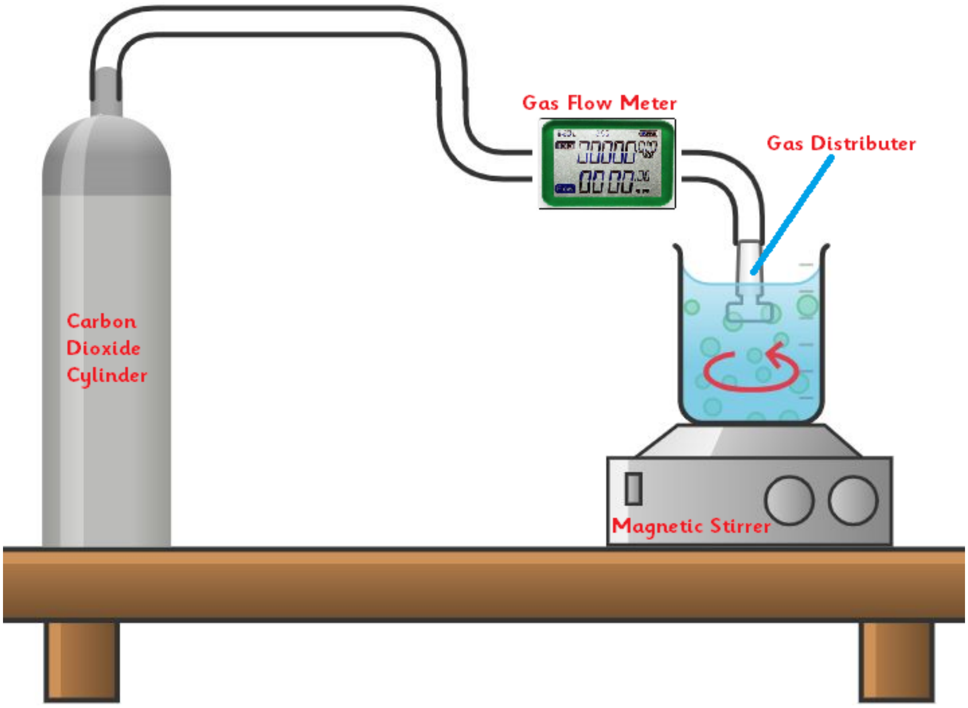

Figure 2. Experimental setup for $CaCO_3$ production.

The glycerol was added to the reaction medium with a certain amount. To produce precipitated calcium carbonate with a smaller particle size in the nano range is very important to slow down the crystal growth. This can be achieved by using a suitable additive that can be adsorbed to the selected sites at the crystal/solution interface and hinder the approach of constituent ions, thereby slowing down the crystal growth in directions perpendicular to the affected faces. Consequently, the relative growth rates of affected and non-affected faces may change [20]. Therefore, glycerol is used as an additive, which can hinder the crystal growth by forming calcium complexes [21].

3. CO_2 gas was bubbled with a certain flow rate which is measured by the "MICRO-FLO PADDLEWHEEL FLOWMETER" for 20 min using a PYREX gas distribution tube with sintered thimble purchased from SciLabware:

- Diameter of tube: 8 mm;
- Nominal overall length: 300 mL;
- OD of thimble: 15 mm;
- Porosity grade: 1.

Popescu et al. [22] suggested a mechanism for the reactions involved in the carbonation of $CaCl_2$ solution in the presence of ammonium hydroxide (NH_4OH) solutions, which can be described by the following steps:

- Absorption of CO_2 gas

$$CO_{2(g)} \rightarrow CO_{2(aq)}; \tag{1}$$

- Formation of hydroxide ion (OH^-)

$$NH_4OH \rightarrow NH_4^+ + OH^-; \tag{2}$$

- Formation of bicarbonate ion

$$CO_{2(aq)} + OH^- \rightarrow HCO_{3\ (aq)}^-; \tag{3}$$

- Formation of carbonate ion

$$HCO_{3\ (aq)}^- + OH^- \rightarrow CO_{3\ (aq)}^{2-} + H_2O; \tag{4}$$

- Formation of $CaCO_3$

$$Ca^{2+}_{(aq)} + CO_{3\ (aq)}^{2-} \rightarrow CaCO_{3(s)}. \tag{5}$$

The chlorine (Cl^-) ions presented may react with (NH_4^+) to yield ammonium chloride (NH_4Cl) that can be used for the preparation of useful fertilizers. Hence, the overall reaction to the above process can be expressed by Equation (6):

$$CaCl_2\ (aq.) + \ H_2O\ + 2NH_4OH(aq.) + \ CO_2(g) \rightarrow CaCO_3(s) + 2NH_4Cl(aq.) \tag{6}$$

4. The resulting product ($CaCO_3$) is allowed to settle, the clear water is withdrawn by filtration, and then the generated particles were allowed to dry naturally.
5. $CaCO_3$ was calcined at 900 °C for 2 h based on previous studies [23,24] and then stored in desiccators to protect the produced calcium oxide which can react with water that is present in the humidity of the air.

2.5. Production of Biodiesel by a Transesterification Reaction Method

The production of biodiesel was done by the following steps:

1. The sunflower oil was added to the round glass batch reactor and heated to the desired reaction temperature using a magnetic stirrer with a heater where the temperature is measured using a thermocouple.
2. The mixture of methanol and biodiesel catalyst (CaO) was added to the heated oil at the indicated reaction temperature. The reflux condenser was attached to one neck for methanol condensation as shown in Figure 3.
3. The reaction mixture was quenched with cooled methanol by the end of the reaction to stop the reaction.
4. The reaction products were filtered to remove the used catalyst.
5. The biodiesel and glycerol were poured into a separating funnel for product separation for 2 h then dried at 80 °C for ma in to remove excess methanol.
6. Biodiesel was then washed with warm (tap water) water to remove the dissolved contaminations like CaO catalyst, methanol, and glycerol, which has a solubility preference in water rather than biodiesel. Thus, contaminations were transferred to lean water and lowered its concentration in biodiesel. The mass transfer was insured by gently mixing of the mixture. Rich water with contaminations were then separated

and replaced by lean water to absorb the remaining contaminations in oil. The washing up was repeated several times until the turbidity of washing water is negligible where water appears transparent having been added to the oil. Transparency of washing water in biodiesel shows that there are no more contaminations to be transferred to water.

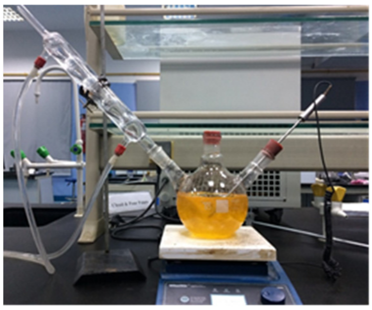

Figure 3. Experimental setup for biodiesel production.

The biodiesel conversion was calculated using Equation (7). The mechanism for the biodiesel production using the transesterification method and CaO catalyst is shown in Figure 4:

$$\text{Biodiesel Conversion, } \% = \frac{\text{Biodiesel Weight}}{\text{SFWCO Weight}} \times 100 \tag{7}$$

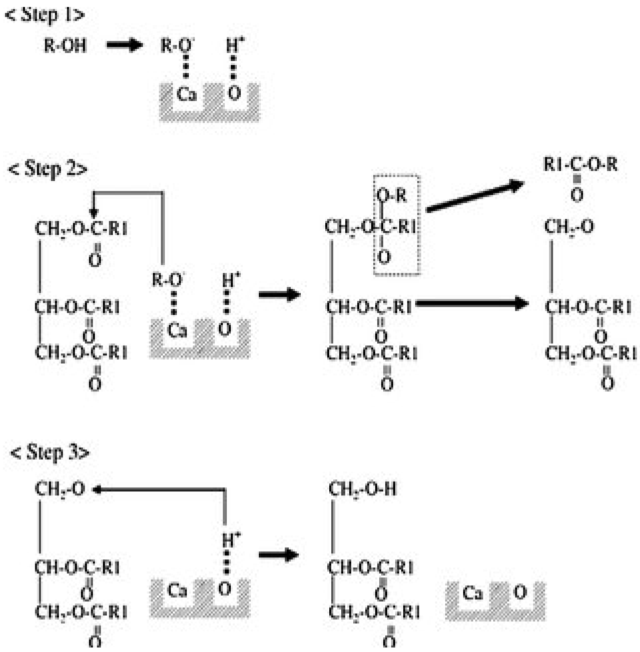

Figure 4. Mechanism of transesterification reaction using CaO catalyst [25].

2.6. Designing Experiments

In this research, response surface methodology was utilized to establish and produce a complete analysis of the impact of reaction variables on reaction responses utilizing experimental design by design expert version 13 [26]. To reduce the number of experimental trials, the central composite design technique (CCD) is applied. Thirty runs were used and the runs 25 to 30 represent the design center. The optimization is done to maximize biodiesel production and minimize its cost.

2.6.1. $CaCO_3$ Production

- The selected reaction responses are the particle size, nm of produced $CaCO_3$, and its yield in percentage.
- The reaction variables are based on Bayoumi et al. [27] as shown in Table 4. Table 5 shows the experimental runs that are generated by the design expert.
- Optimization was done by minimizing the particle size and maximizing the production yield of $CaCO_3$, while minimizing the stirring rate.

Table 4. Design of experiment matrix for CaC_3.

Parameter	**Unit**	**Values**	
		−1	**1**
Stirring rate	rpm	500	1300
CO_2 gas flow rate	mL/min	900	2000
Amount of ammonia	mL	15	35
Volume of glycerol	mL	0	25

Table 5. $CaCO_3$ experimental runs.

Run No.	**Stirring Rate, rpm**	**CO_2 Gas Flow Rate, mL/min**	**Amount of Ammonia, mL**	**The Volume of Glycerol, mL**
1	500	900	15	0
2	1300	900	15	0
3	500	2000	15	0
4	1300	2000	15	0
5	500	900	35	0
6	1300	900	35	0
7	500	2000	35	0
8	1300	2000	35	0
9	500	900	15	25
10	1300	900	15	25
11	500	2000	15	25
12	1300	2000	15	25
13	500	900	35	25
14	1300	900	35	25
15	500	2000	35	25
16	1300	2000	35	25
17	100	1450	25	12.5
18	1700	1450	25	12.5
19	900	350	25	12.5
20	900	2550	25	12.5
21	900	1450	5	12.5
22	900	1450	45	12.5
23	900	1450	25	0
24	900	1450	25	37.5
25–30	900	1450	25	12.5

2.6.2. Biodiesel Production

- The selected reaction response is biodiesel yield;
- The reaction variables are based on Al-Sakkari et al. [13] as shown in Table 6. Table 7 shows the experimental runs that are generated by the design expert.
- Optimization was done by maximizing the production yield of biodiesel while minimizing the reaction time and temperature.

Table 6. Design of experiment matrix for biodiesel production.

Parameter	Unit	Values	
		−1	**1**
Reaction time	h	2	6
Methanol to oil molar ratio	-	9	15
CaO catalyst loading concentration	%	1	5
Stirring rate	°C	50	70

Table 7. Biodiesel experimental runs.

Run No.	Temperature, °C	Catalyst Loading, %	Methanol/Oil Ratio	Reaction Time, h
1	50	1	9	2
2	50	1	9	6
3	50	1	15	2
4	50	1	15	6
5	50	5	9	2
6	50	5	9	6
7	50	5	15	2
8	50	5	15	6
9	70	1	9	2
10	70	1	9	6
11	70	1	15	2
12	70	1	15	6
13	70	5	9	2
14	70	5	9	6
15	70	5	15	2
16	70	5	15	6
17	60	3	12	0
18	60	3	12	8
19	60	3	6	4
20	60	3	18	4
21	60	1	12	4
22	60	7	12	4
23	40	3	12	4
24	80	3	12	4
25–30	60	3	12	4

2.7. Investigations Done on the Optimal Biodiesel Sample

The resulted biodiesel optimum sample was tested using the following methods:

1. Physicochemical properties determination and comparison with both EN14214 [28] European Biodiesel Standard, and ASTM D6751 [29], International Standard.
2. Gas chromatography (GC) that tests the sample according to the standards EN 14103 [30] and EN14105 [31] methods.

2.8. CaO Reusability

The optimum biodiesel sample that resulted from the first reaction use with biodiesel conversion equals approximately 96%, being filtered and reacted with glycerol to remove the methanol molecules from the catalyst and then reused again and again without adding any new solid waste at the optimum reaction conditions. The biodiesel conversion was calculated at each use as an indication for the catalyst strength determination.

3. Results and Discussion

3.1. Mineralogical Analysis of Produced $CaCO_3$ and the Biodiesel Catalyst

3.1.1. $CaCO_3$ Mineralogical Analysis

The mineralogical investigation in Figure 5 reveals that it is primarily composed of the calcite ($CaCO_3$) phase, with a trace of cristobalite (SiO_2). This confirmed that the $CaCO_3$ is produced by the $CaCO_3$ process, which is expected to be produced by the chemical reaction.

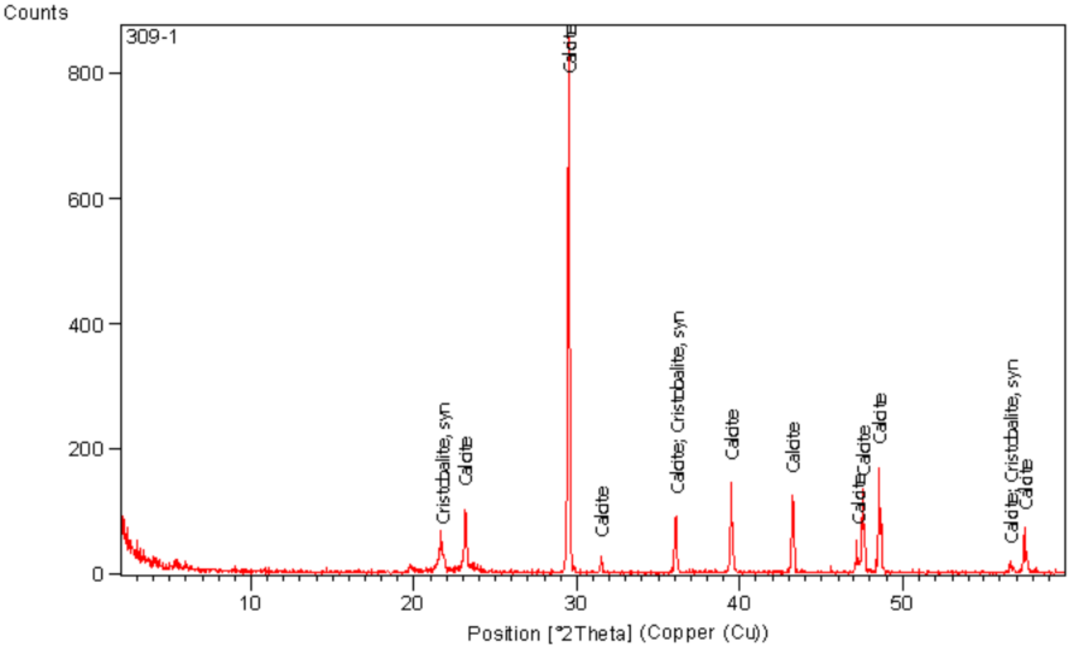

Figure 5. Mineralogical analysis of produced $CaCO_3$.

3.1.2. Mineralogical Analysis of Biodiesel Catalyst (CaO)

Figure 6 shows the XRD pattern of CaO and the peaks list of the reference sample (pure calcium oxide) in blue. X-ray diffraction analysis proved that it consists almost exclusively of CaO. The peak positions and relative intensities of the biodiesel catalyst and reference data are an excellent match. This proved that the decomposition of $CaCO_3$ to CaO is completed at approximately 100% since the only present phase is CaO with no $CaCO_3$ phase.

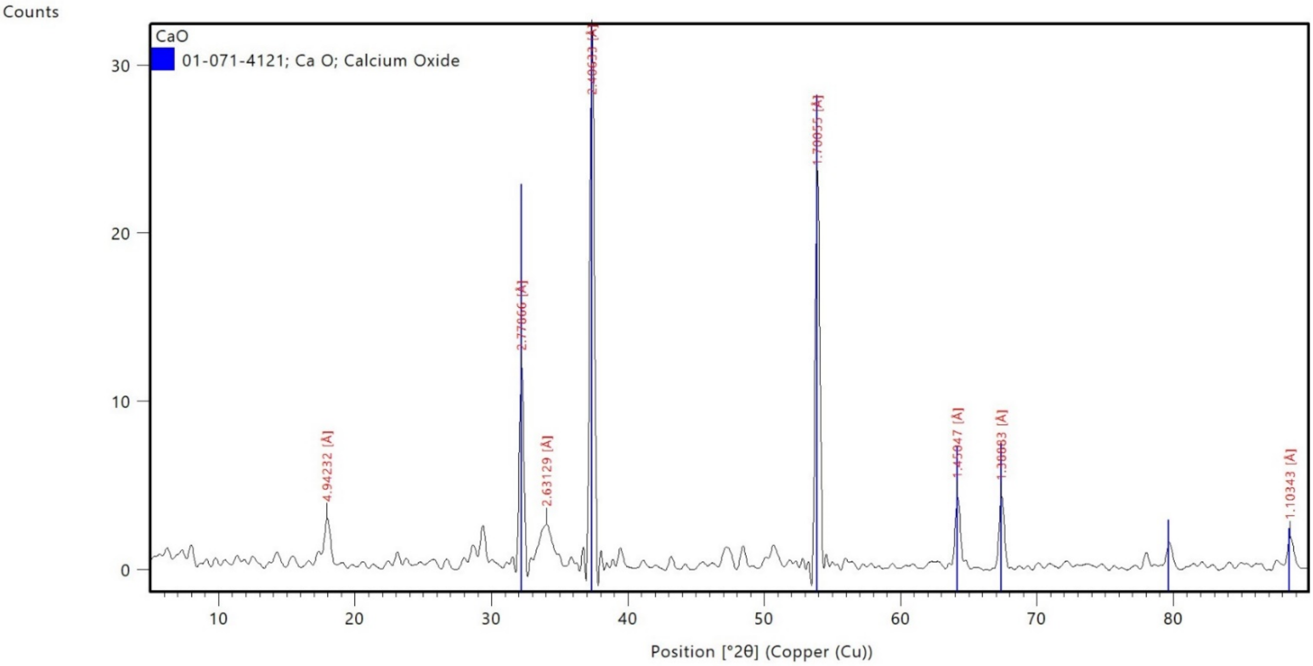

Figure 6. Mineralogical analysis of CaO including the peaks list of CaO and the reference sample.

3.2. SEM Results of CaO

The SEM analysis of the used biodiesel catalyst is shown in Figure 7. According to SEM pictures, the generated CaO catalyst is irregular in shape, porous in structure, and contains active sites. In other words, there were a variety of particle sizes and shapes, indicating that the catalyst has a larger surface area for reaction. This gives a good indication that this catalyst will be active and give biodiesel with a high yield and with a low used amount of catalyst.

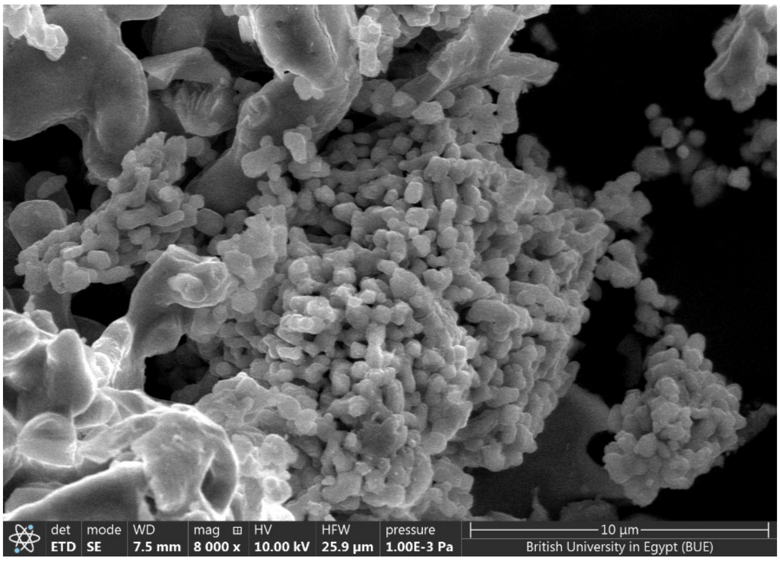

Figure 7. SEM of biodiesel catalyst (CaO).

3.3. Screen Analysis of Biodiesel Catalyst (CaO)

The particle size distribution of calcium oxide is shown in Figure 8. The catalyst is so fine, as shown in this diagram. The average particle size was 0.56 µm. This low particle size means a high surface area, which is confirmed by the SEM result.

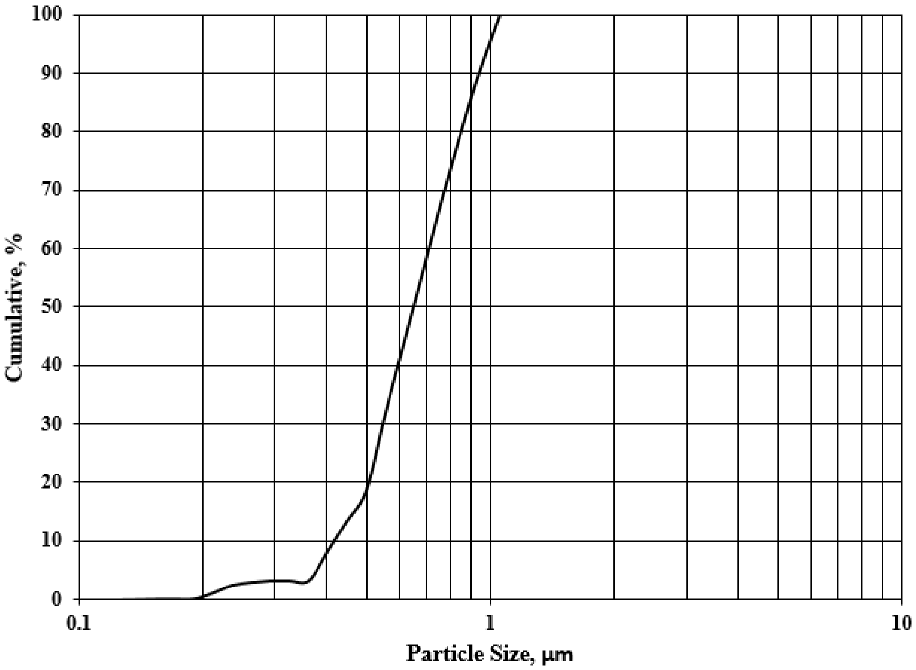

Figure 8. Cumulative screen analysis curve of biodiesel catalyst (CaO).

3.4. Analysis of the Products

Design Expert was used to create the regression model. At a 95% confidence level or 5% significance level, analysis of variance (ANOVA) was employed to assess the significance of the resulting model. The *p*-values should be less than 0.05. The critical F value for the resulting model can be determined using the number of variables, sample size, and significance level, and then compared with the F values for the model to determine the significance of the model.

3.5. $CaCO_3$ Analysis

The particle size and yield of $CaCO_3$ were calculated. The findings of the ANOVA analysis performed by the design expert program are shown in Tables 8 and 9. The following equations illustrate the relationship between particle size, the yield of produced $CaCO_3$, and reaction conditions using a simplified quadratic model:

$$X = 0.202B - 0.083A - 10.276C - 14.975D - 0.008BD + 0.466CD + 0.273D^2 + 696.495 \tag{8}$$

$$Y = 0.009A + 0.008B + 0.02C + 0.009D + 0.00001AB + 48 \times 10^{-6}B^2 + 52.373 \tag{9}$$

where X is the particle size of produced $CaCO_3$ in nm or the first reaction response while Y is the yield of produced $CaCO_3$ in percentage, A is stirring rate in rpm, B is CO_2 gas flow rate in mL/min, C is the amount of ammonia in mL, and D is the amount of glycerol in mL.

Table 8. ANOVA analysis table for response 1: particle size of $CaCO_3$.

Source	Sum of Squares	df	Mean Square	F-Value	*p*-Value
Model	5.345×10^5	7	76,351.81	11.59	<0.0001
A-Stirring rate	26,169.01	1	26,169.01	3.97	0.0588
B-Flow rate of CO_2 gas	79,637.76	1	79,637.76	12.09	0.0021
C-Amount of ammonia	47,481.51	1	47,481.51	7.21	0.0135
D-Amount of glycerol	2.286×10^5	1	2.286×10^5	34.70	<0.0001
BD	45,956.64	1	45,956.64	6.97	0.0149
CD	54,347.27	1	54,347.27	8.25	0.0089
D^2	52,232.72	1	52,232.72	7.93	0.0101
Residual	1.450×10^5	22	6589.16		
Lack of Fit	1.450×10^5	17	8527.15		
Pure Error	0.0000	5	0.0000		

Table 9. ANOVA analysis table for response 2: $CaCO_3$ Yield.

Source	Sum of Squares	df	Mean Square	F-Value	*p*-Value
Model	4453.22	6	742.20	385.19	<0.0001
A-Stirring rate	2562.67	1	2562.67	1329.97	<0.0001
B-Flow rate of CO_2 gas	1734.00	1	1734.00	899.91	<0.0001
C-Amount of ammonia	0.9600	1	0.9600	0.4982	0.4874
D-Amount of glycerol	0.3151	1	0.3151	0.1635	0.6897
AB	100.00	1	100.00	51.90	<0.0001
B^2	55.28	1	55.28	28.69	<0.0001
Residual	44.32	23	1.93		
Lack of Fit	44.32	18	2.46		
Pure Error	0.0000	5	0.0000		

The predicted values were compared to the experimental results as shown in Figures 9 and 10. As demonstrated in the figures, the plot exhibits reasonable agreement and excellent correlation.

3.6. Biodiesel Analysis

The biodiesel was produced, and the conversion rate was determined. Table 10 shows the results of the ANOVA analysis done by the design expert program. The following equation shows a relationship between biodiesel conversion and reaction conditions using a simplified quadratic model:

$$Z = 0.748E + 11.891F + 2.835G + 5.328H - 0.193FG - 0.086FH - 0.181F^2 - 0.03H^2 - 174.215 \quad (10)$$

where Z stands for biodiesel conversion, E stands for reaction time in hours, F stands for methanol to oil ratio, G stands for catalyst loading in weight percent, and H stands for reaction temperature in degrees Celsius.

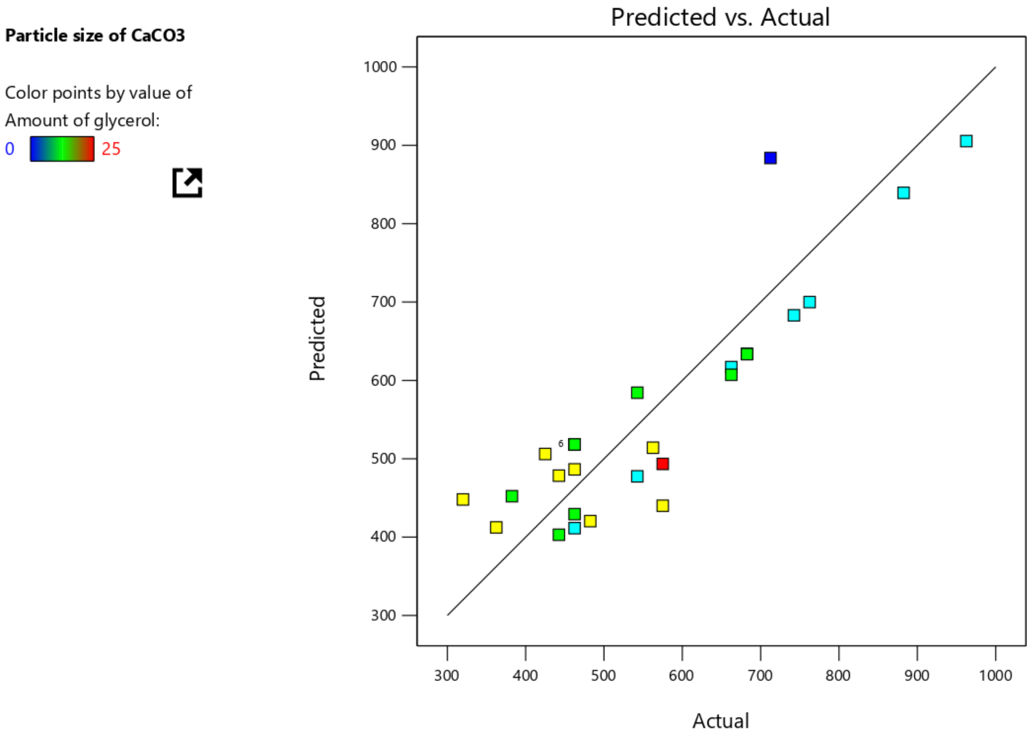

Figure 9. $CaCO_3$ particle size relationship between expected and experimental results.

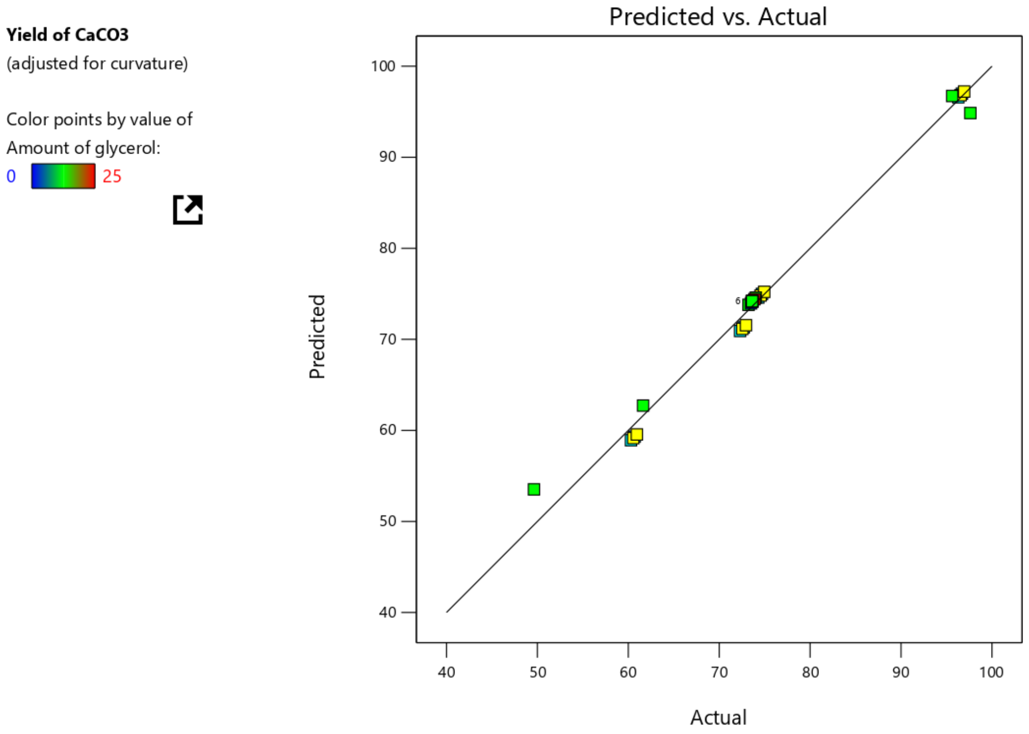

Figure 10. $CaCO_3$ yield relationship between expected and experimental results.

Table 10. Biodiesel conversion ANOVA analysis.

Source	Sum of Squares	df	Mean Square	F-Value	*p*-Value
Model	2246.30	8	280.79	68.16	<0.0001
E-Reaction Time	53.76	1	53.76	13.05	0.0016
F-Methanol/oil ratio	671.72	1	671.72	163.06	<0.0001
G-Catalyst loading	25.74	1	25.74	6.25	0.0208
H-Temperature	1057.82	1	1057.82	256.78	<0.0001
FG	21.49	1	21.49	5.22	0.0329
FH	108.47	1	108.47	26.33	<0.0001
F^2	75.35	1	75.35	18.29	0.0003
H^2	259.22	1	259.22	62.92	<0.0001
Residual	86.51	21	4.12		
Lack of Fit	86.51	16	5.41		
Pure Error	0.0000	5	0.0000		

The predicted values were compared to the experimental results. As demonstrated in Figure 11, this graph exhibits excellent agreement.

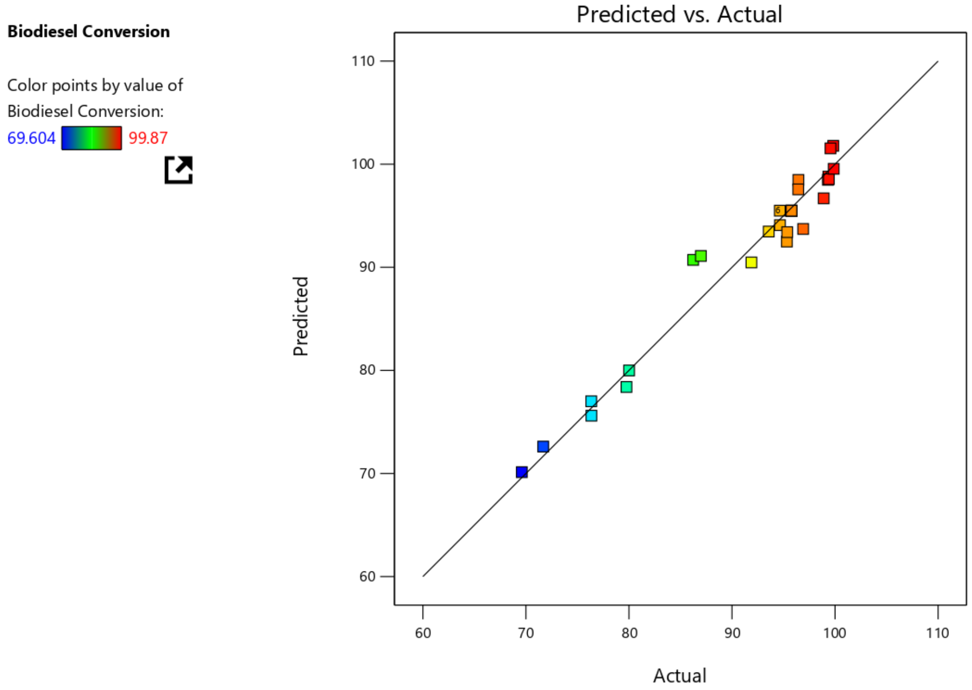

Figure 11. Relationship between biodiesel predicted yield and experimental results.

3.7. Reaction Conditions Effect on the Particle Size and the Yield of $CaCO_3$

The effect of the stirring rate, CO_2 flow rate, ammonia amount, and glycerol amount on the particle size and yield of $CaCO_3$ is depicted in Figures 12 and 13. The amount of glycerol has the greatest impact on the particle size of $CaCO_3$ while the stirring rate and the flow rate of CO_2 have the greatest impact on the $CaCO_3$ yield.

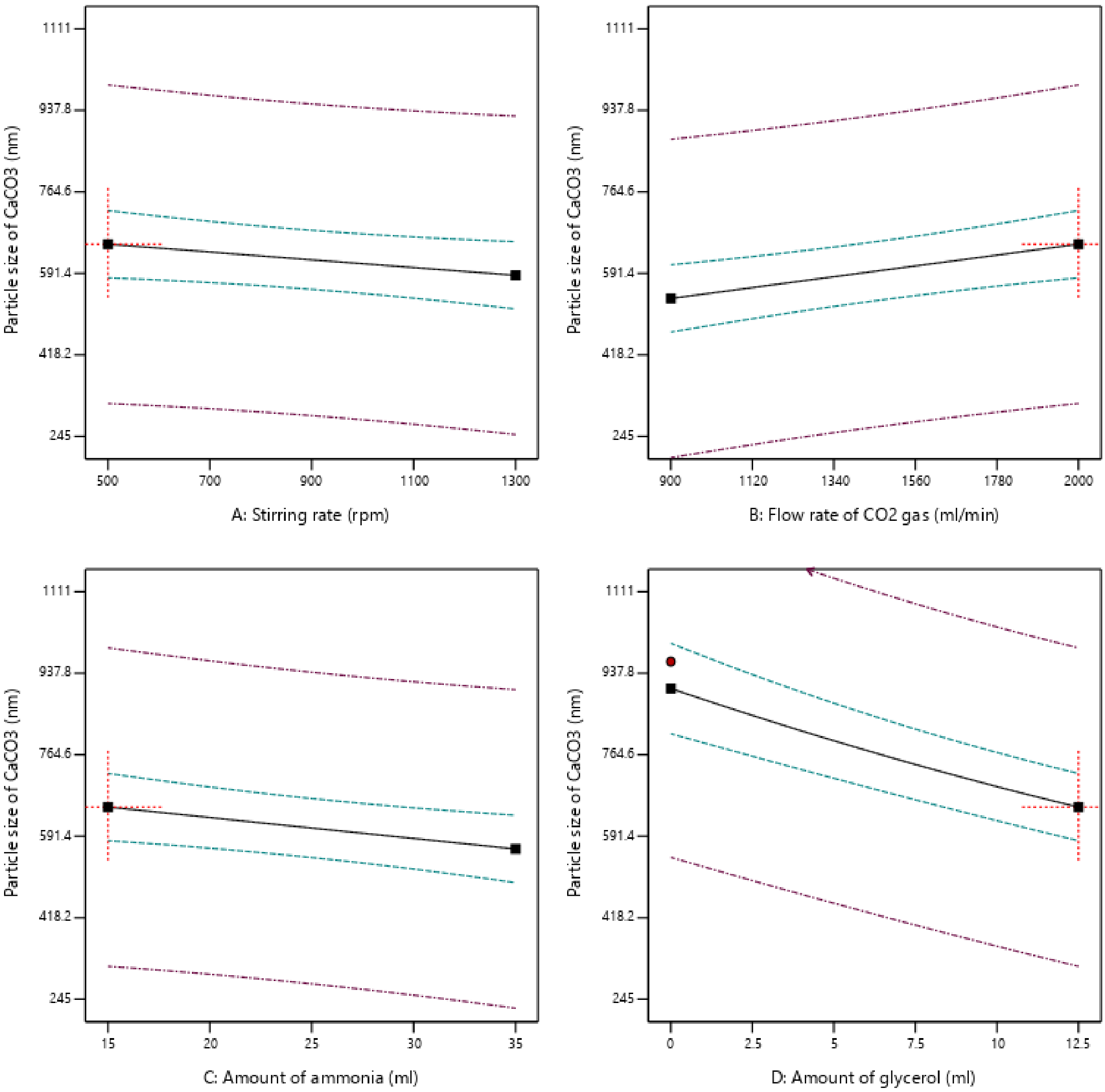

Figure 12. Process variables affect the $CaCO_3$ particle size.

3.7.1. Effect of Stirring Rate on the Particle Size and the Yield of $CaCO_3$

The average particle size appears to decrease as the stirring rate increases. Because of the high mass transfer resistance, operation at low stirring rates results in a local accumulation of super-saturation, which facilitates the development of agglomerated particles and hence a bigger particle size. High stirring rates, on the other hand, improve gas–liquid mass transfer because the stirring velocities can overcome the high mass transfer barrier in this case. This slows the agglomeration process and allows to produce smaller particles [32].

An increase in the stirring rate resulted in a rise in yield. This extremely small monotonic rise in yield could point to a reduction in mass transfer resistance. This reduction may have aided the process, increasing the reaction yield.

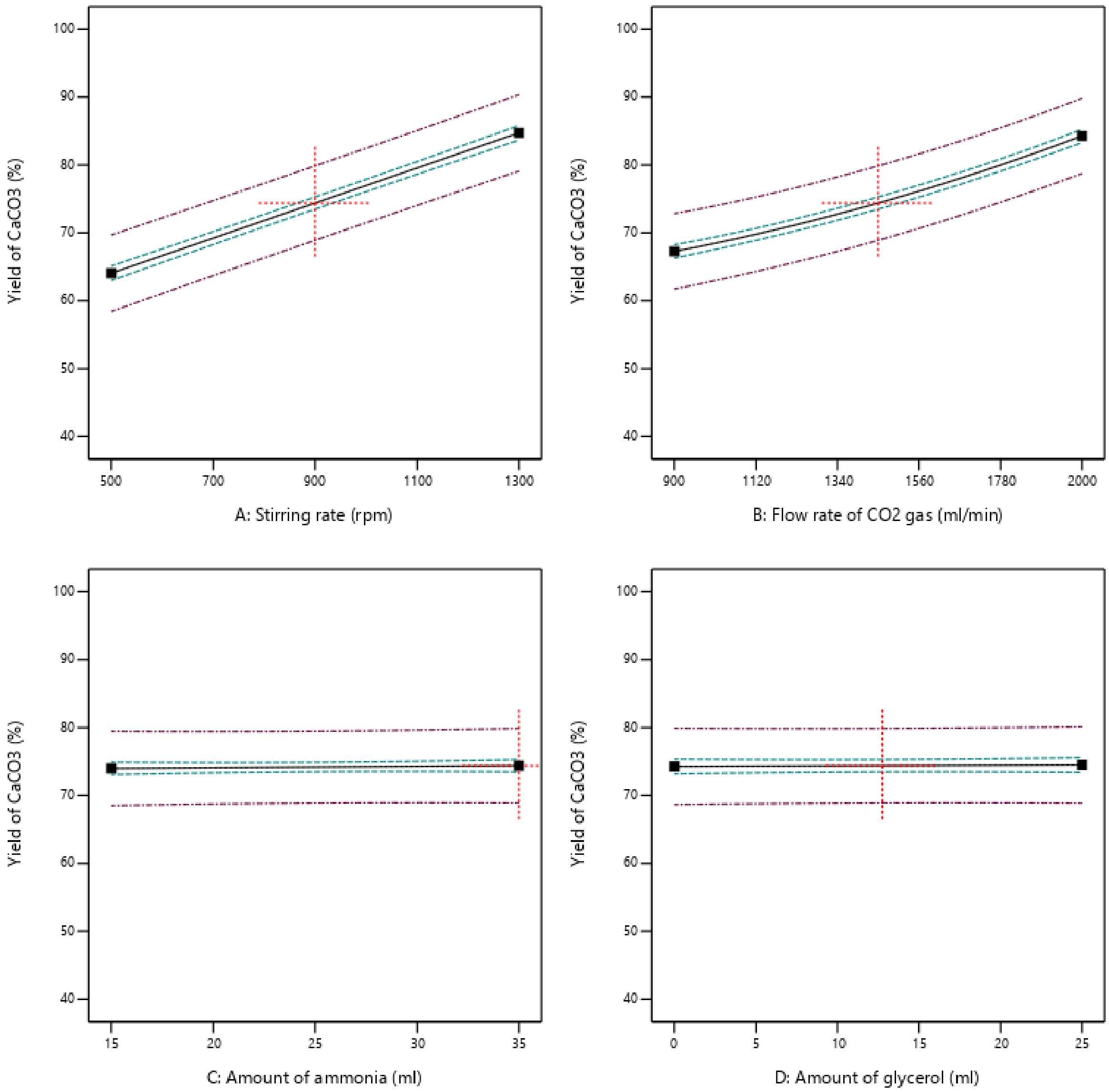

Figure 13. Process variables affect the $CaCO_3$ yield.

3.7.2. Effect of the Amount of Ammonia on the Particle Size and the Yield of $CaCO_3$

It was discovered that, as the amount of ammonia added to the mixture grows, the particle size of the resulting product decreases. Considering the entire reaction equation, this discovery makes sense (Equation (6). According to this equation, increasing the amount of ammonium hydroxide will shift the reaction to the forward direction, resulting in a high degree of calcium carbonate super-saturation, leading to a large rise in the nucleation rate, and therefore the creation of smaller sized PCC particles [33].

The amount of ammonia used in the reaction has a minor impact on the product yield. Because ammonia can extract the chloride from calcium chloride, but CO_2 cannot, the reaction cannot proceed without it. The Le Chatelier principle strongly supports this theory, as increasing the amount of ammonia shifts the reaction to the forward direction, increasing the amount of product.

3.7.3. Effect of the Gas Flow Rate on the Particle Size and the Yield of $CaCO_3$

The following is an explanation for CO_2 behavior: at low CO_2 gas flow rates, the amount of CO_2 provided is insufficient to react with all calcium ions present in the solution, resulting in calcium ion accumulation inside the solution. Due to the adsorption of these positively charged ions on the surface of the negatively charged $CaCO_3$ crystals, the presence of excess Ca^{2+} would result in increased particle size, lowering the repulsion forces between crystals and causing particle agglomeration [34]. Any increase in the gas volumetric flow rate causes a significant rise in the gas–liquid mass transfer rate, resulting in an increase in the nucleation rate and a decrease in the particle size of $CaCO_3$ [33].

The CO_2 gas is used in the reaction, and its flow rate has a significant impact on the product yield. Increasing the gas flow rate, according to Le Chatelier's principle, will shift the reaction to the forward direction, increasing the amount of product produced.

3.7.4. Effect of the Amount of Glycerol on the Particle Size and the Yield of $CaCO_3$

As the glycerol percentage rises, the particle size falls. The creation of an adsorption layer on the surface of $CaCO_3$ particles could explain this. Adsorbed molecules are oriented perpendicular to the $CaCO_3$ surface and OH^- groups are connected to the surface if the concentration of surface-active molecules of the organic additive is sufficient. As a result of the presence of three OH^- groups, glycerol can form a well-organized layer. However, at high glycerol concentrations, the medium's viscosity rises, affecting the mass transfer coefficient and causing inefficient mass transfer, resulting in the creation of big particles [35].

As expected, the addition of glycerol has no influence on the product yield. The yield is exclusively affected by the reactants in the process; glycerol is merely an external component utilized to control particle size.

3.8. Reaction Conditions Effect on the Yield of Biodiesel

The temperature of the reaction and the M:O ratio has the biggest influence on biodiesel conversion as indicated in Figure 14, which shows the influence of each reaction parameter on biodiesel conversion.

3.8.1. Effect of the Reaction Temperature on the Yield of Biodiesel

Reaction temperature is an important variable for biodiesel production. Consequently, the reaction temperature has been chosen within a range of 50 to 70 °C to investigate the effect of wide range of excess methanol on the biodiesel conversion. It observed that increasing temperature will greatly increase the biodiesel yield. Increasing reaction temperature will increase the reaction rate or velocity, which increases the biodiesel yield.

3.8.2. Effect of the Reaction Time on the Yield of Biodiesel

Reaction time is an important variable for biodiesel production. Consequently, the reaction time has been chosen within a range of 1 to 4 h to investigate the effect of wide range of reaction time on the biodiesel yield. Increasing the reaction time will give more time for the reaction to happen, which will increase the biodiesel yield.

3.8.3. Effect of the Methanol to Oil Ratio on the Yield of Biodiesel

M:O molar ratio is an important variable for biodiesel production. According to the stoichiometric equation of trans-esterification reaction, three moles of methanol are required to convert 1 mole of oil to 3 moles of biodiesel. This illustrates the importance of excess methanol, which has an important role in maintaining the reaction at constant rate and enhancing forward reaction. Consequently, the M:O molar ratio has been chosen within a range of 9:1 to 15:1 to investigate the effect of wide range of excess methanol on the biodiesel conversion. It observed that the yield of biodiesel greatly increases with the increase in the methanol to oil ratio.

3.8.4. Effect of the Catalyst Loading on the Yield of Biodiesel

CaO weight percentage is an important variable for biodiesel production. Consequently, CaO weight percentage has been chosen within a range of 1 to 5% to investigate the effect of wide range of excess methanol on the biodiesel conversion. It was observed that the catalyst loading has a low or approximately no effect on the biodiesel yield, which means that a minimum amount of catalyst will give the required result, as this catalyst is a strong one.

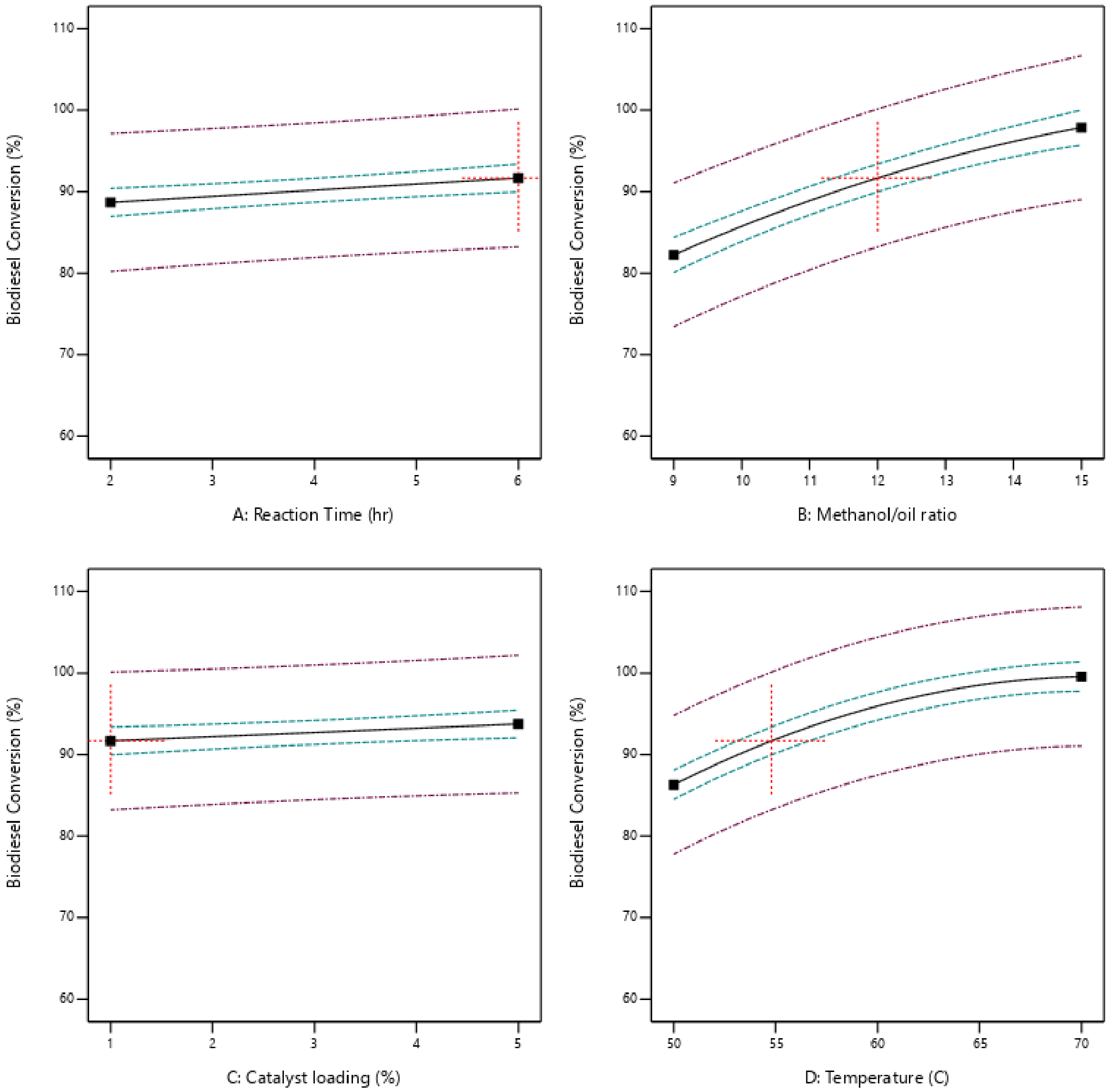

Figure 14. Process variables affect the yield of biodiesel.

3.9. Reaction Response Variation with the Variables' Interactions

Figure 15 indicates the relationship between the CO_2 flow rate, amount of glycerol, and the particle size of $CaCO_3$. Figure 16 indicates the relationship between the amount of ammonia, the amount of glycerol, and the particle size of $CaCO_3$. Figure 17 indicates the relationship between the CO_2 flow rate, stirring rate, and the yield of $CaCO_3$. Figure 18 indicates the relationship between the catalyst loading, methanol to oil ratio, and the yield of biodiesel. Figure 19 indicates the relationship between the reaction temperature, methanol to oil ratio, and the yield of biodiesel.

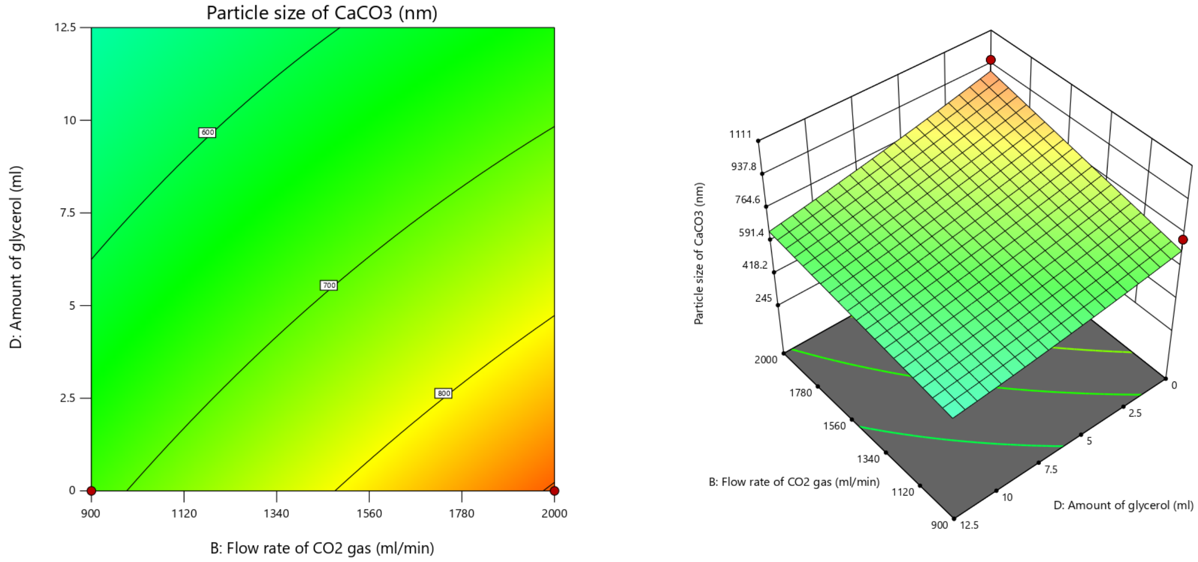

Figure 15. Relationship between the CO_2 flow rate, amount of glycerol, and the particle size of $CaCO_3$ (Contour and 3D plot).

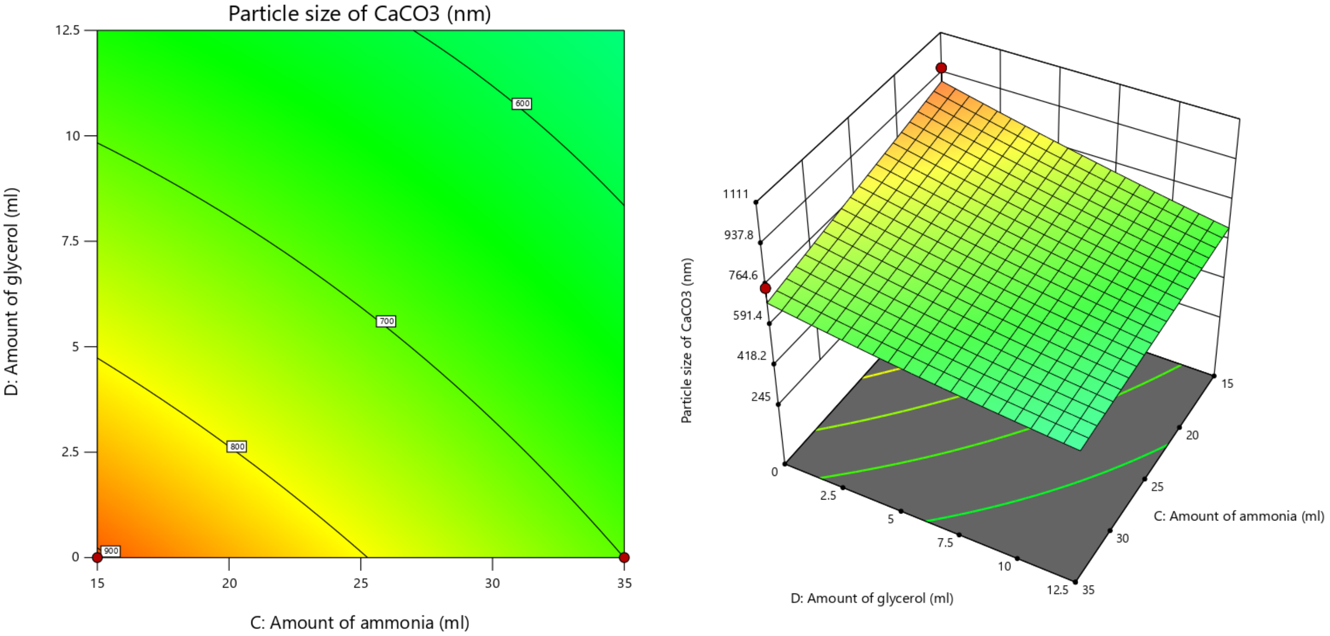

Figure 16. Relationship between the amount of ammonia, amount of glycerol, and the particle size of $CaCO_3$ (Contour and 3D plot).

3.10. Process Optimization

Many solutions were developed by the design expert, but the solution with the highest desirability was selected as an optimum solution. The optimization process was done in two steps as follows.

3.10.1. $CaCO_3$ Production Process Optimization

Targets of the independent variables have been set based on minimizing the particle size of $CaCO_3$ while increasing its yield to be able to get a highly active catalyst with a high amount. Table 11 shows the optimum results for $CaCO_3$ production processes.

Table 11. Optimization results.

Stirring Rate, rpm	The Flow Rate of CO_2 Gas, mL/min	Amount of Ammonia, mL	Amount of Glycerol, mL	The Particle Size of Produced $CaCO_3$, nm	The Yield of $CaCO_3$, %	Desirability
1300	2000	15	25	420.4	96.8	0.911

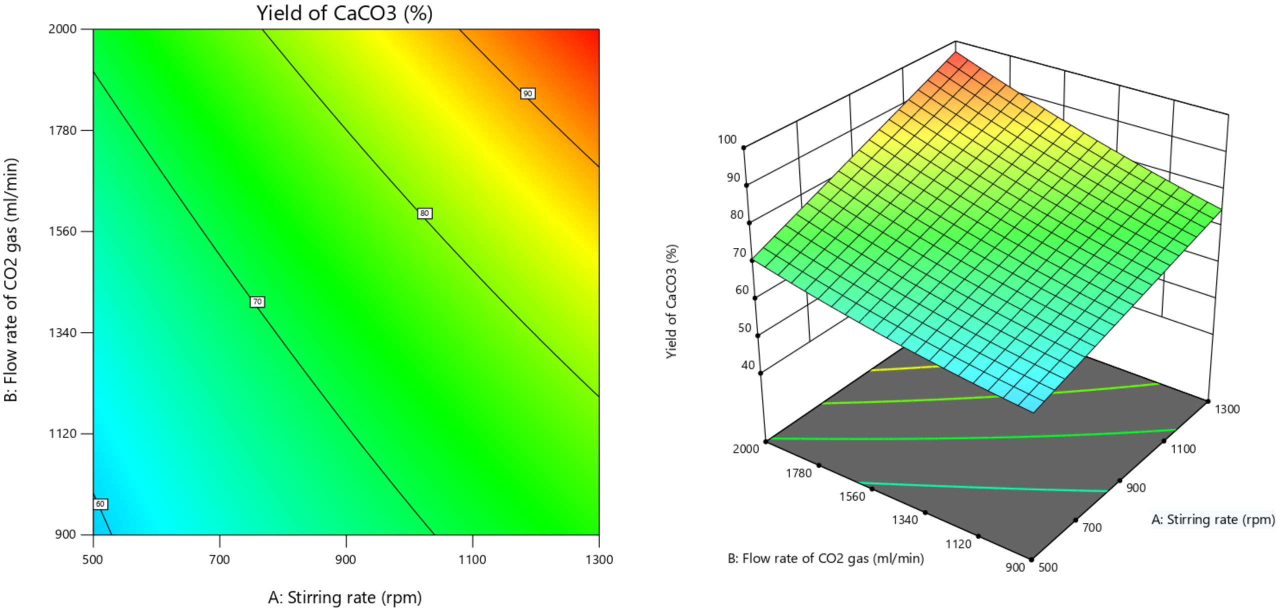

Figure 17. Relationship between the CO_2 flow rate, stirring rate, and the yield of $CaCO_3$ (Contour and 3D plot).

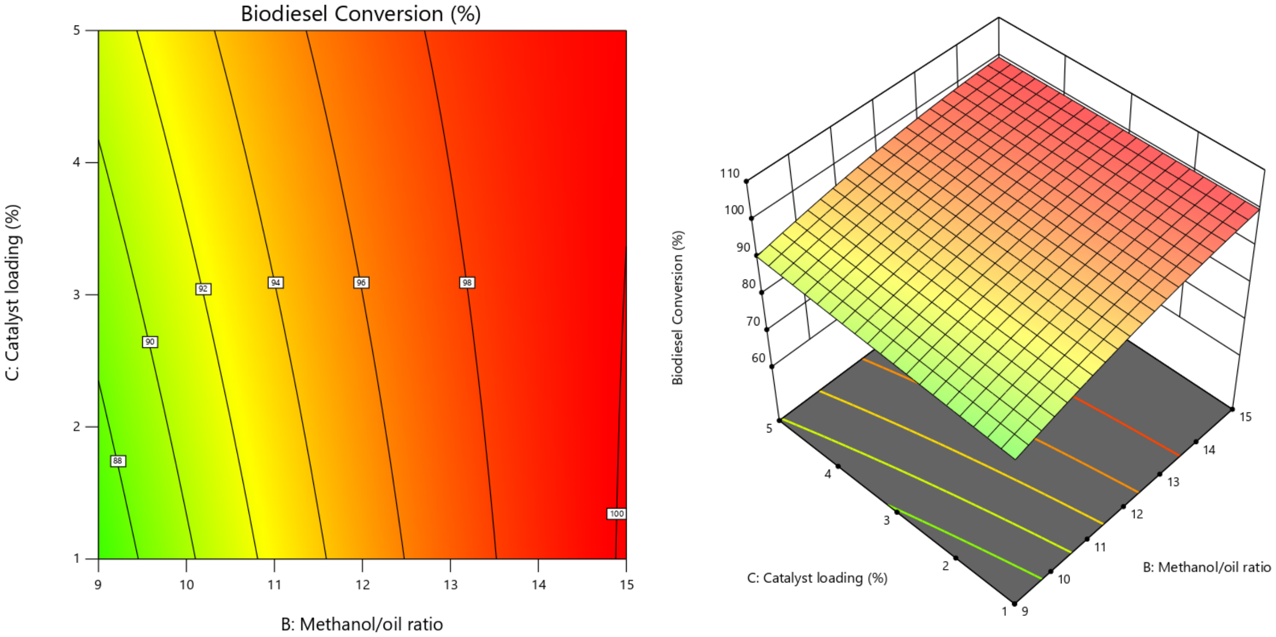

Figure 18. Relationship between the catalyst loading, methanol to oil ratio, and the yield of biodiesel (Contour and 3D plot).

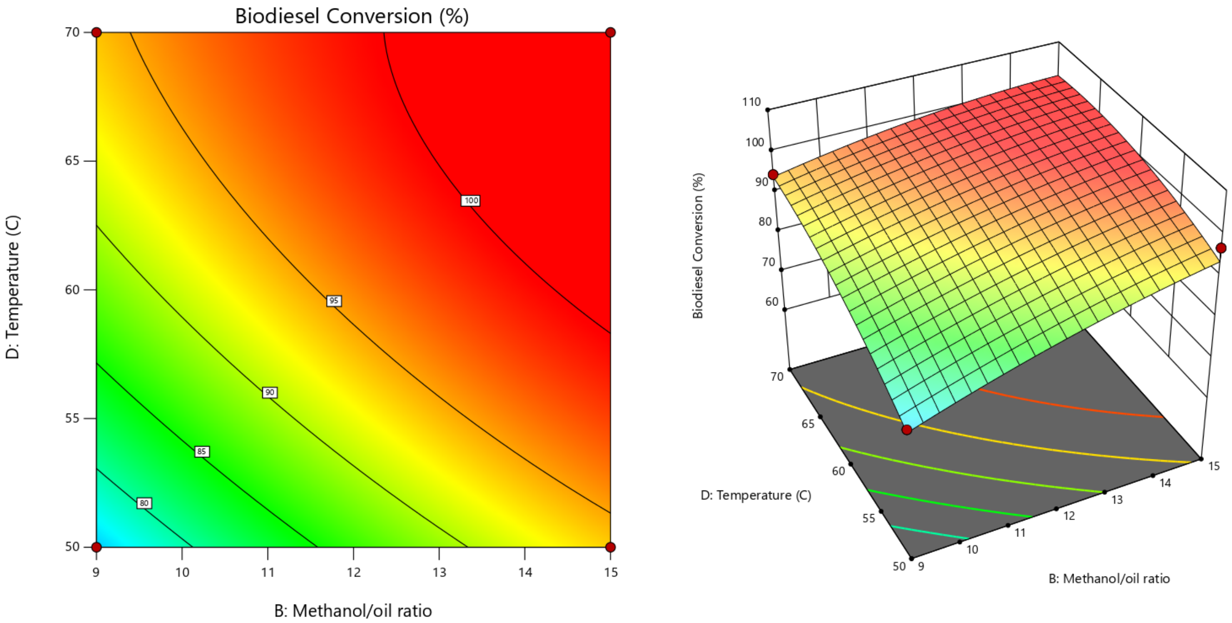

Figure 19. Relationship between the reaction temperature, methanol to oil ratio, and the yield of biodiesel (Contour and 3D plot).

3.10.2. Biodiesel Production Process Optimization

Targets of the independent variables have been set based on environmental and economic considerations. For the highly energy consuming variables including temperature and time, they have been set to be minimized with high importance (5th degree of importance). Finally, the response variable, which is the biodiesel yield, has been set to be maximized to achieve the highest biodiesel yield within the independent variables' target restrictions. Table 12 shows the optimum results for biodiesel production processes.

Table 12. Optimization results.

Methanol/Oil Ratio	Temperature, °C	Catalyst Loading, %	Reaction Time, h	Biodiesel Conversion, %	Desirability
15	56	1	2.000	95.8	0.765

3.11. *Optimum Biodiesel Sample Analysis*

Table 13 lists the physicochemical parameters and their standard limits. EN14214 [28] and ASTM D 6751 [29] both agree on all of the characteristics required for biodiesel.

Table 13. The optimal biodiesel sample's physicochemical characteristics.

Test	Results	Standard Method	EN14214	ASTM D6751
Calorific value (MJ/kg)	39.821	ASTM D-5865 [36]	>32.9	
Flashpoint (°C)	170	ASTM D-93 [37]	>101	>130
Pour point (°C)	−22	ASTM D-97 [38]		
Density at 15 °C (g/cm^3)	0.8851	ASTM D-4052 [39]	0.86–0.9	
Cloud point (°C)	−13	ASTM D-97 [38]	<−4	
Kinematic viscosity at 40 °C (cSt)	4.6	ASTM D-445 [40]	3.5–5.0	1.9–6.0

Table 14 summarizes the results of the optimum biodiesel sample's gas chromatography examination (GC). EN 14103 [30] and EN 14105 [31] European standards are in agreement with the findings.

Table 14. GC results.

Composition		Results	Specification
Total FAME		97.6%	More than 96.5%
Glycerides	Tri-	0.0856%	Less than 0.2%
	Di-	0.0078%	Less than 0.2%
	Mono-	0.0043%	Less than 0.8%
Glycerol	Total	0.019%	Less than 0.25%
	Free	0.01%	Less than 0.02%

3.12. CaO Reusability

Figure 20 demonstrates that conversion falls from 96 percent after the first usage to the third use. One of the associated problems with the catalyst's lower activity is glycerol contamination on the active site. The second reason is that active CaO is slaking into less active carbonate, bicarbonate, and hydroxide compounds forming in addition to 1% catalyst loading that is used. This means it is used with a very low amount, so it is worth nothing to recycle the catalyst or search for any method for catalyst recycling.

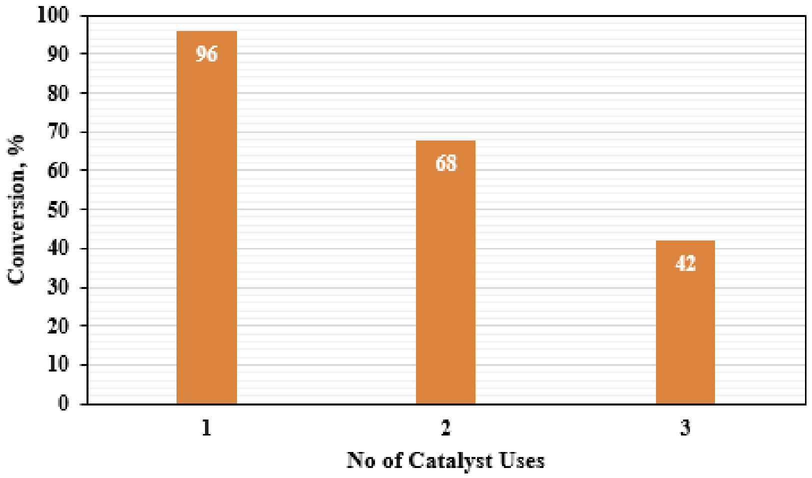

Figure 20. Reusability test results.

4. Optimum Biodiesel Production from Solvay Wastewater

The concentration of $CaCl_2$ is not low as its value is 115 kg/m^3 according to Table 1, and the factory produced a large amount of wastewater each day. Soda ash production by the Solvay process produced a waste stream of 10 m^3 per ton of product Na_2CO_3. This stream, known as distiller waste, contains $CaCl_2$, NaCl, and small quantities of $Ca(OH)_2$ and $CaCO_3$ [41]. This stream is discharged into the Mediterranean Sea, which may cause environmental problems, and it is suggested to recover $CaCl_2$ present in this stream and produce valuable products such as $CaCO_3$. According to the amount of wastewater produced every day, the CaO can be produced and used in biodiesel production as its loading in the biodiesel reaction is 1%, so it is used with a small amount so there is no need for additional raw materials. Regarding the energy consumption cost, it will be totally covered by the cost of produced biodiesel, so this process is a profitable process.

This research can be done in real-life by adding a new unit to the factory that produces $NaCO_3$ (soda ash) using the Solvay process method to get the use of valuable chemicals in its wastewater before throwing it as shown in Figure 21. The wastewater is used to produce $CaCO_3$, then firing to produce CaO, and then finally the biodiesel production step. The following steps show the summary for all experimental procedures done on a lab scale with the optimum conditions for all reaction or process parameters. Process upgrading can be done to make this process done on industrial scale.

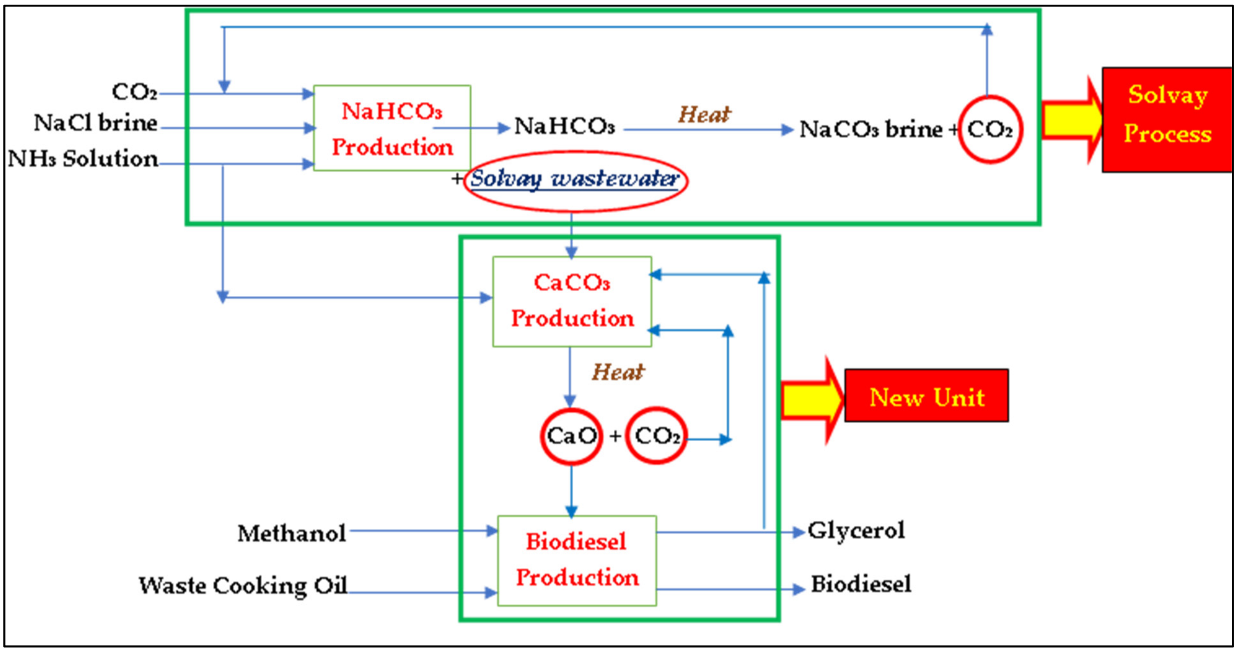

Figure 21. Optimum biodiesel production process utilizing Solvay wastewater, CO_2, and waste cooking oil.

4.1. $CaCO_3$ Production Step

1. Mixing Solvay wastewater with ammonia solution using a mixing ratio 3 (ammonia solution): 47 (wastewater).
2. Adding glycerol to the reaction mixture with an amount equal to 10% of the total volume of the mixture.
3. Stirring the resulted solution mixture using 1300 rpm rotational speed on a magnetic stirrer.
4. Bubbling CO_2 gas with a flowrate of 2000 mL/min using a gas distributer for 20 min.
5. By the end of the reaction, the product was filtered to get the resulting $CaCO_3$ with 420.4 nm particle size and 96.8% yield.

4.2. CaO Production Step

$CaCO_3$ was calcined at 900 °C for 2 h and then stored in desiccators to protect the produced calcium oxide which can react with water that is present in the humidity of the air.

4.3. Biodiesel Production Step

1. Purification and drying for the waste sunflower waste cooking oil.
2. Heating the resulted biodiesel in a round bottom flask at 56 °C using a magnetic stirrer with a heater.
3. Mixing methanol and biodiesel catalyst with the hot oil with 15 methanol to oil ratio and 1% catalyst loading.
4. Leaving the reaction mixture for 2 h and then quenching with cold methanol to stop the reaction. Then, the products were left to cool.
5. Separating the products using a separating funnel for 2 h.
6. Drying the resulting products at 80 °C for half an hour to remove the methanol.
7. Biodiesel washing to remove any contaminations in it.

8. By the end of these steps, the resulting biodiesel has 95.8% conversion.

5. Comparison between This Research and the Previous Ones

The comparison shown in Table 15 shows the differences between the results obtained by this research and other published papers. This research has many important benefits and advantages as shown in the following:

- Low energy consumption because of using a low reaction compared with others.
- High biodiesel conversion.
- Biodiesel catalyst generation from Solvay wastewater, CO_2, and waste cooking oil.
- High used methanol to oil ratio. The extra methanol is separated from the resulting biodiesel by distillation and then recycled and reused.
- Low amount of used catalyst compared with the other studies so its separation after the reaction is easier.

Table 15. Comparison of the results of this research and the previous ones.

Study	Used Catalyst	Catalyst Preparation	Reaction Conditions				Biodiesel Conversion	Reference
			Methanol/Oil Ratio	Catalyst Loading	Reaction Temperature	Reaction Time		
1	CaO from Eggshell	Need	12:1	3.5 wt%	60 °C	2 h	92%	[42]
2	Technical grade CaO	Do not need	7.1:1	5.9 wt%	65 °C	2 h	92.6%	[43]
	CaO from eggshells	Need	7:1	6 wt%	65 °C	2.2 h	91.4%	
3	CaO from Limestone	Need	6:1	5 wt%	65 °C	4 h	86%	[44]
4	CaO, industrial grade	Do not need	8.72:1	8.75 wt%	60 °C	2 h	98.5%	[45]
5	Nano-CaO	Do not need	11:1	3.675 wt%	60 °C	2 h	97.61%	[46]
6	Nano-CaO	Do not need	15:1	5 wt%	65 ± 2 °C	3 h	88.87%	[47]
7	CaO is Solvay wastewater	Need	15:1	1 wt%	56 °C	2 h	95.8%	(Present work)

6. Conclusions

Biodiesel was produced from waste sunflower oil and methanol in the presence of CaO as a heterogeneous catalyst. Solvay wastewater was used as a source for CaO. Waste cooking oil, wastewater, and CO_2, which are considered dangerous materials to the environment, are used to produce a valuable product, so this research has an environmental benefit and economic benefit because of using waste materials as a replacement for raw materials. Four independent reaction conditions were selected to detect their impact on biodiesel production: reaction temperature, methanol to oil (M:O) molar ratio, reaction time, and catalyst loading, and another four independent reaction conditions were selected to detect their impact on particle size and the yield of $CaCO_3$: CO_2 flowrate, amount of glycerol, amount of ammonia, and stirring rate. The response surface approach was used to assess the impact of all reaction factors on biodiesel output. Three models were developed to describe the relationship between the reaction responses and reaction variables. The design expert program developed the optimum reaction responses and reaction variables, which resulted in an optimum biodiesel production process. This research has an economic benefit. This research aims to produce the maximum amount of biodiesel using minimum energy and low reaction conditions. The best conditions were found to be an M:O molar ratio of 15:1, a catalyst dosage of 1%, a reaction temperature of 56 °C, a reaction period of 2 h, and a stirring rate of 750 rpm, yielding a biodiesel conversion of 95.8 percent that agreed with the international standards of biodiesel. The reusability test revealed that it recommended to not reuse CaO again after the first use, and there is no problem as CaO is used in the biodiesel production with a small amount.

Author Contributions: Conceptualization, M.H.R.; Data curation, R.A.B.; Formal analysis, M.H.R.; Investigation, R.A.B.; Methodology, M.H.R.; Supervision, M.H.R.; Validation, M.H.R.; Writing—original draft, M.H.R.; Writing—review and editing, M.H.R. All authors have read and agreed to the published version of the manuscript.

Funding: The authors declare that this paper is not funded by any funding agency.

Data Availability Statement: All data generated or analyzed during this study are available in this article.

Acknowledgments: M. H. Roushdy, the first author, wishes to express her heartfelt gratitude to Magdi F. Abadir of Cairo University.

Conflicts of Interest: The authors declare that they have no known competing financial interests or personal relationships that could have appeared to influence the work reported in this paper.

References

1. Habibullah, M.; Masjuki, H.H.; Kalam, M.A.; Rahman, S.M.A.; Mofijur, M.; Mobarak, H.M.; Ashraful, A.M. Potential of biodiesel as a renewable energy source in Bangladesh. *Renew. Sustain. Energy Rev.* **2015**, *50*, 819–834. [CrossRef]
2. Ayoola, A.A.; Fayomi, O.S.I.; Adegbite, O.A.; Raji, O. Biodiesel Fuel Production Processes: A Short Review. *IOP Conf. Ser. Mater. Sci. Eng.* **2021**, *1107*, 012151. [CrossRef]
3. Khodary, K.E.; Naeem, M.M.; Roushdy, M.H. Utilization of electric arc furnace dust as a solid catalyst in biodiesel production. *Clean Technol. Environ. Policy* **2021**. [CrossRef]
4. Chintagunta, A.D.; Zuccaro, G.; Kumar, M.; Kumar, S.P.J.; Garlapati, V.K.; Postemsky, P.D.; Kumar, N.S.S.; Chandel, A.K.; Simal-Gandara, J. Biodiesel Production From Lignocellulosic Biomass Using Oleaginous Microbes: Prospects for Integrated Biofuel Production. *Front. Microbiol.* **2021**, *12*, 658284. [CrossRef]
5. Lamichhane, G.; Khadka, S.; Adhikari, S.; Koirala, N.; Poudyal, D.P. Biofuel Production from Waste Cooking Oils and its Physicochemical Properties in Comparison to Petrodiesel. *Nepal J. Biotechnol.* **2020**, *8*, 87–94. [CrossRef]
6. Shankar, S.; Shikha. *Renewable and Nonrenewable Energy Resources: Bioenergy and Biofuels*; Principles and Applications of Environmental Biotechnology for a Sustainable Future book series; Springer: Singapore, 2017; pp. 293–314.
7. De Blasio, C. Processes of Bioethanol Production. In *Fundamentals of Biofuels Engineering and Technology. Green Energy and Technology*; Springer: Singapore, 2019. [CrossRef]
8. Pasha, M.K.; Dai, L.; Liu, D.; Guo, M.; Du, W. An overview to process design, simulation and sustainability evaluation of biodiesel production. *Biotechnol. Biofuels* **2021**, *14*, 129. [CrossRef]
9. Roushdy, M.H. Heterogeneous Biodiesel Catalyst from Steel Slag Resulting from an Electric Arc Furnace. *Processes* **2022**, *10*, 465. [CrossRef]
10. Thangaraj, B.; Solomon, P.R.; Muniyandi, B.; Ranganathan, S.; Lin, L. Catalysis in biodiesel production—A review. *Clean Energy* **2019**, *3*, 2–23. [CrossRef]
11. Watcharathamrongkul, K.; Jongsomjit, B.; Phisalaphong, M. Calcium oxide based catalysts for ethanolysis of soybean oil. *Songklanakarin J. Sci. Technol.* **2010**, *32*, 627–634.
12. Sai Bharadwaj, A.V.S.L.; Singh, M.; Niju, S.; Meera Sheriffa Begum, K.M.; Anantharaman, N. Biodiesel production from rubber seed oil using calcium oxide derived from eggshell as catalyst-optimization and modeling studies. *Green Processing Synth.* **2019**, *8*, 430–442. [CrossRef]
13. Al-Sakkari, E.G.; El-Sheltawy, S.T.; Abadir, M.F.; Attia, N.K.; El-Diwani, G. Investigation of cement kiln dust utilization for catalyzing biodiesel production via response surface methodology. *Int. J. Energy Res.* **2017**, *41*, 593–603. [CrossRef]
14. Çalban, T.; Kavci, E. Removal of calcium from soda liquid waste containing calcium chloride. *Energy Sources Part A: Recovery Util. Environ. Eff.* **2010**, *32*, 407–418. [CrossRef]
15. Czaplicka, N.; Konopacka-Łyskawa, D. Studies on the utilization of post-distillation liquid from Solvay process to carbon dioxide capture and storage. *SN Appl. Sci.* **2019**, *1*, 431. [CrossRef]
16. Czaplicka, N.; Konopacka-Łyskawa, D. Utilization of gaseous carbon dioxide and industrial ca-rich waste for calcium carbonate precipitation: A review. *Energies* **2020**, *13*, 6239. [CrossRef]
17. Rasouli, H.; Esmaeili, H. Characterization of MgO nanocatalyst to produce biodiesel from goat fat using transesterification process. *3 Biotech* **2019**, *9*, 429. [CrossRef]
18. *ASTM E 11-09*; Standard Specification for Woven Wire Test Sieve Cloth and Test Sieves. ASTM International: West Conshohocken, PA, USA, 2010; Volume 1, p. 9.
19. Degfie, T.A.; Mamo, T.T.; Mekonnen, Y.S. Optimized Biodiesel Production from Waste Cooking Oil (WCO) using Calcium Oxide (CaO) Nano-catalyst. *Sci. Rep.* **2019**, *9*, 18982. [CrossRef]

20. Varma, S.; Chen, P.; Unnikrishnan, G. Gas-liquid reactive crystallization for the synthesis of $CaCO_3$ nanocrystals. *Mater. Chem. Phys.* **2011**, *126*, 232–236. [CrossRef]
21. Westin, K.J.; Rasmuson, Å.C. Crystal growth of aragonite and calcite in presence of citric acid, DTPA, EDTA and pyromellitic acid. *J. Colloid Interface Sci.* **2005**, *282*, 359–369. [CrossRef]
22. Popescu, M.-A.; Isopescu, R.; Matei, C.; Fagarasan, G.; Plesu, V. Thermal decomposition of calcium carbonate polymorphs precipitated in the presence of ammonia and alkylamines. *Adv. Powder Technol.* **2014**, *25*, 500–507. [CrossRef]
23. Widayat, W.; Darmawan, T.; Hadiyanto, H.; Rosyid, R.A. Preparation of Heterogeneous CaO Catalysts for Biodiesel Production. *J. Phys. Conf. Ser.* **2017**, *877*, 012018. [CrossRef]
24. Singh, N.B.; Singh, N.P. Formation of CaO from thermal decomposition of calcium carbonate in the presence of carboxylic acids. *J. Therm. Anal. Calorim.* **2007**, *89*, 159–162. [CrossRef]
25. Widiarti, N.; Nimah Yatim, L.; Bahruji, H.; Prasetyoko, D. Development of CaO From Natural Calcite as a Heterogeneous Base Catalyst in the Formation of Biodiesel: Review. *J. Renew. Mater.* **2019**, *7*, 915–939. [CrossRef]
26. Montgomery, D.C. *Montgomery Design and Analysis of Experiments*, 8th ed.; Arizona State University: Tempe, AZ, USA, 2013; Volume 2009, 2001p.
27. Bayoumi, R.A.; Ahmed, T.S.; Soliman, A.; Ismail, I.M. Nano Calcium Carbonate Production Utilizing Solvay-Process Industrial Wastewater and Carbon Dioxide. *Key Eng. Mater.* **2019**, *821*, 350–358. [CrossRef]
28. *EN 14214:2013 V2+A1*; Liquid Petroleum Products—Fatty Acid Methyl Esters (FAME) for Use in Diesel Engines and Heating Applications—Requirements and Test Methods. European Committee for Standardization: Brussels, Belgium, 2013; p. 14538.
29. *D6751-15c A*; Standard Specification for Biodiesel Fuel Blend Stock (B100) for Middle Distillate Fuels. ASTM International: West Conshohocken, PA, USA, 2010; pp. 1–11.
30. Biodiesel, A. *APPLICATION NOTE EN 14103 Determination of Total FAME and Linolenic Acid Methyl Ester in FAME with AC Biodiesel All in One Solution*; AC Analytical Controls, PAC L.P.: Houston, TX, USA, 2011; pp. 1–3.
31. Biodiesel, A.; Glycerol, T. *APPLICATION NOTE EN 14105 Determination of Free and Total Glycerol and Mono-, Di—Triglycerides in Fatty Acid Methyl Esters (FAME)*; SCION Instruments: Livingston, UK, 2011; pp. 2–4.
32. Scmeme, C.E. Effect of gas-liquid mass transfer on crystal size distribution during the batch precipitation of calcium carbonate. *Chem. Eng. Sci.* **1991**, *46*, 3289–3293.
33. Sun, B.-C.; Wang, X.-M.; Chen, J.-M.; Chu, G.-W.; Chen, J.-F.; Shao, L. Synthesis of nano-$CaCO_3$ by simultaneous absorption of CO_2 and NH_3 into $CaCl_2$ solution in a rotating packed bed. *Chem. Eng. J.* **2011**, *168*, 731–736. [CrossRef]
34. Jung, W.M.; Kang, S.H.; Kim, K.S.; Kim, W.S.; Choi, C.K. Precipitation of calcium carbonate particles by gas-liquid reaction: Morphology and size distribution of particles in Couette-Taylor and stirred tank reactors. *J. Cryst. Growth* **2010**, *312*, 3331–3339. [CrossRef]
35. Konopacka-Łyskawa, D.; Kościelska, B.; Karczewski, J. Effect of some organic solvent–water mixtures composition on precipitated calcium carbonate in carbonation process. *J. Cryst. Growth* **2015**, *418*, 25–31. [CrossRef]
36. Mahapatra, D. A Review on Steam Coal Analysis—Calorific Value. *Am. Int. J. Res. Sci.Technol. Eng. Math.* **2016**, *14*, 143–152.
37. Products, P. *Astm D93 Flash Point*; ASTM International: West Conshohocken, PA, USA, 2004; p. 80112.
38. Edition, F. *Final Draft Uganda Standard*; ASTM International: West Conshohocken, PA, USA, 2013.
39. *D40052-15*; Standard Test Method for Density, Relative Density, and API Gravity of Liquids by Digital Density Meter. ASTM International: West Conshohocken, PA, USA, 2013; pp. 1–8.
40. *ASTM D445-06*; Standard Test Method for Kinematic Viscosity of Transparent and Opaque Liquids (and Calculation of Dynamic Viscosity). In *Manual on Hydrocarbon Analysis*, 6th ed; ASTM International: West Conshohocken, PA, USA, 2008; pp. 1–10.
41. Alamdari, A.; Alamdari, A.; Mowla, D. Kinetics of calcium carbonate precipitation through CO_2 absorption from flue gas into distiller waste of soda ash plant. *J. Ind. Eng. Chem.* **2014**, *20*, 3480–3486. [CrossRef]
42. Erchamo, Y.S.; Mamo, T.T.; Workneh, G.A.; Mekonnen, Y.S. Improved biodiesel production from waste cooking oil with mixed methanol–ethanol using enhanced eggshell-derived CaO nano-catalyst. *Sci. Rep.* **2021**, *11*, 6708. [CrossRef] [PubMed]
43. Ayoola, A.A.; Fayomi, O.S.I.; Adeeyo, O.A.; Omodara, J.O.; Adegbite, O. Impact assessment of biodiesel production using CaO catalyst obtained from two different sources. *Cogent. Eng.* **2019**, *6*, 1615198. [CrossRef]
44. Vivi Sisca, S.; Zilfa, J.N. Biodiesel Production from Waste Cooking Oil Using Catalyst Calcium Oxide Derived of Limestone Lintau Buo. *Arch. Pharm. Pract.* **2020**, *11*, 8–14.
45. Soria-Figueroa, E.; Mena-Cervantes, V.Y.; García-Solares, M.; Hernández-Altamirano, R.; Vazquez-Arenas, J. Statistical optimization of biodiesel production from waste cooking oil using CaO as catalyst in a Robinson-Mahoney type reactor. *Fuel* **2020**, *282*, 118853. [CrossRef]
46. Bharti, P.; Singh, B.; Dey, R.K. Process optimization of biodiesel production catalyzed by CaO nanocatalyst using response surface methodology. *J. Nanostruct. Chem.* **2019**, *9*, 269. Available online: link.gale.com/apps/doc/A607973452/AONE?u=anon~{}f1b9196&sid=googleScholar&xid=fe3eb596 (accessed on 14 May 2022). [CrossRef]
47. Abd Malek, M.N.F.; Pushparaja, L.; Hussin, N.M.; Embong, N.H.; Bhuyar, P.; Rahim, M.H.A.; Maniam, G.P. Exploration of efficiency of nano calcium oxide (CaO) as catalyst for enhancement of biodiesel production. *J. Microbiol. Biotechnol. Food Sci.* **2021**, *11*, e3935. [CrossRef]